# Reliability Analysis of Litzka Castellated Beams

Washington B. Vieira[1], André L. R. Brandão[1], Giovanne de L. Santana[1]

[1]*Institute of Integrated Engineering, Federal University of Itajubá*
*Itabira, 35.903-087, Minas Gerais, Brazil*
vieira@unifei.edu.br, andreriqueira@unifei.edu.br, d2021006903@unifei.edu.br

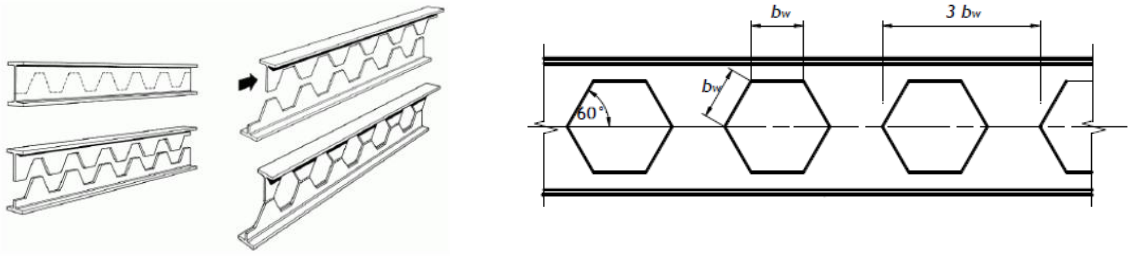
**Abstract.** This paper presents a safety evaluation of Litzka castellated beams, based on calculation models proposed in technical literature. It is noteworthy that there are currently no applicable Brazilian standards or official design criteria for this type of structure. The safety assessment is carried out through structural reliability analysis of the beams and advanced finite element-based analysis of their actual resistance. The effects of geometric imperfections and residual stress on the resistance of the beams are considered. Statistical parameters related to model error, material strength, geometric properties, and permanent and variable loads are considered in the reliability evaluation. Reliability indices are obtained for load combinations according to Brazilian, American, and European standards. These indices reflect the safety level of the beams designed according to the analyzed models. The results are compared with target reliability indices recommended by ASCE and Eurocode.

**Keywords:** castellated beams; Litzka; numerical model; finite element method; structural reliability.

## 1 Introduction

Steel construction advanced in the early 20th century with the introduction of electric welding, enabling lighter structural systems with greater span capacity and sufficient stiffness to limit displacements within design limits. In beams, performance is governed by flexural stiffness and strength, with cross-sectional geometry often optimized to maximize the inertia-to-weight ratio. In many cases, design is controlled by deflection limits, requiring increased stiffness without additional strength.

Castellated steel beams (CSB) are an effective solution in this context. They are fabricated from rolled I-sections, longitudinally cut in specific patterns; the halves are offset and welded to form a deeper beam with web openings (Fig. 1a). Several typologies exist, varying according to the cutting pattern, which affects the spacing and angle of the openings relative to the beam's longitudinal axis. The most common patterns are Anglo-Saxon, Litzka, and Peiner. The Litzka pattern (Fig. 1b), which is the focus of this study, features regular hexagonal openings spaced at three times the web post width.




(a) (b)

Figure 1. CSB: (a) fabrication procedure (Grünbauer [1]); (b) Litzka pattern (Vieira [2]).

Reliability of the web-post buckling strength model proposed by Vieira [2] is assessed using the First-Order Reliability Method (FORM), providing design guidance for Litzka-type castellated beams.

# 2 Literature Review

## 2.1 Castellated Steel Beams

Castellated steel beams (CSB) originated in Europe around 1930 due to demand for deeper sections than standard rolled I-profiles. They are fabricated by longitudinally cutting rolled I-sections along a specific pattern, allowing the halves to be shifted and welded, resulting in a deeper beam with successive web openings (Veríssimo et al. [3]). The geometry of CSB provides visual lightness, allows utility passage, and can increase member strength, making them suitable for floors and roof systems (Oliveira et al. [4]).

The increase in steel strength over recent decades has heightened the significance of instability in compressed elements, necessitating a reassessment of failure modes (Vieira [5]). Web openings increase slenderness, introduce free edges, and cause abrupt inertia variations, altering the structural behavior compared to solid-web beams (Gonçalves et al. [6]).

Figure 2 presents the geometric properties of the cross-section of a rolled I-profile and a castellated I-profile. The design length is denoted by $L_v$.



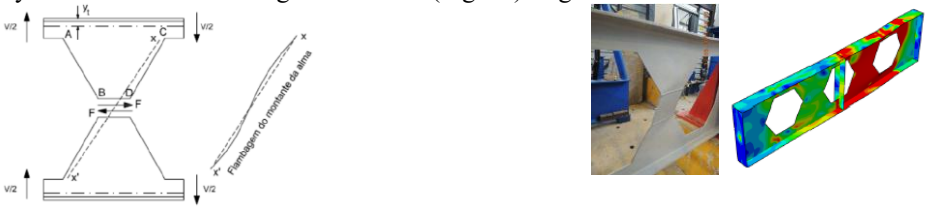

Figure 2. Geometric elements: I-section and CSB section (Veríssimo, et al. [7]; Oliveira [8])

From the original profile height ($d$) other geometric parameters of castellated beams can be derived. The castellated profile height ($d_g$) is related to the original profile height by the expansion ratio $k = d_g/d$, denominada de razão de expansão. Additional geometric properties of interest are shown in Fig. 2: $b_w$ is the width of the intermediate web posts, $b_{we}$, the width of the end web post, $b$ the horizontal projection of the inclined side of the opening, $a_o$ the width of the opening, $p$ the pitch, and $h_o$ the opening height (Pereira et al. [9]).

## 2.2 Web-post buckling (WPB).

The presence of openings in CSB results in a distinct structural behavior compared to solid web steel beams. By increasing the web height without changing its thickness, slenderness is increased, while the free edges of the openings become more susceptible to local instabilities [2]. The main failure modes are plastic bending mechanism, lateral-torsional buckling, Vierendeel mechanism, local flange buckling, and web-post buckling.

In the case of web-post buckling (WPB), the web post of a CSB is subjected to internal forces as shown in Fig. 3. The shear force F along the welded joint causes tension along edge AB of the web post, while edge CD is subjected to compressive stresses, which may lead to WPB. When WPB occurs, the lateral displacement is accompanied by rotation around the diagonal line xx' (Fig. 3a). Fig. 3b shows a CSB that failed due to WPB.




(a) (b)

Figure 3. WPB: (a) rotation about the diagonal *xx'* (Kerdal and Nethercot [10]); (b) lateral displacement [2].

Vieira [2] proposed a calculation model that allows estimating the load-carrying capacity of CSB under the WPB, with application in both elastic and inelastic regimes. The general equation is given by Eq. (1):

$$V = \gamma_o \chi V_p. \quad (1)$$

Where $\gamma_o$ is an adjustment factor that accounts for the error of the analytical model relative to the numerical one, and of the numerical model relative to the experimental results; $V_p$ is the plastic shear force, and $\chi$ is the dimensionless shear force factor.

For the models in which the equations of the Litzka pattern were developed, the value of $\gamma_o$ proposed in [2] is taken as 1.25, or a modified version obtained from updated numerical results, presented in eq. (2). The plastic shear force is given by eq. (3).

$$\gamma_o = 2 \cdot \sqrt[4]{\frac{d_g}{L_v}}. \quad (2)$$

$$V_p = 1.609 b_w y_o \left(\frac{t_w}{p}\right)^{1,223} f_y. \quad (3)$$

Where $y_o$ is the distance between the centroid of the flange and the beam axis, and $f_y$ is the steel yield strength.

The value of $\chi$ is equal to 1 when $\lambda < \lambda_p$, equal to $\chi_{inel}$ when $\lambda_p < \lambda < \lambda_r$, or equal $\chi_{cr}$ when $\lambda > \lambda_r$. The value of the slenderness index $\lambda$ and the slenderness limits $\lambda$p e $\lambda_r$ are given by the following equations:

$$\lambda_p = 241.12 - 6.5524 \sqrt{\frac{E}{f_y}}. \quad (4)$$

$$\lambda = \frac{l_e \sqrt{12}}{t_w}. \quad (6)$$

$$\lambda_r = 10.998 \sqrt{\frac{E}{f_y}} - 60.640. \quad (5)$$

$$l_e = K \frac{\sqrt{b_w^2 + h_o^2}}{2}. \quad (7)$$

Where $K = 1.0$ for profiles without a cover plate, or $K = (h_o + h_p)/h_o$ for the general case.

The values of $\chi_{cr}$ and $\chi_{inel}$ are given by the following equations:

$$\chi_{cr} = 27.515 \left(\frac{E}{f_y}\right)^{0.947} \left(\frac{1}{\lambda}\right)^{1.830}. \quad (8)$$

$$\chi_{inel} = \frac{\lambda_r - \chi_r \lambda_p}{\lambda_r - \lambda_p} - \frac{\chi_p - \chi_r}{\lambda_r - \lambda_p} \lambda. \quad (9)$$

Where $\chi_p = 1$ and $\chi_r$ is equal to $\chi_{cr}$ obtained from eq. (8), using $\lambda = \lambda_r$.

### 2.3 Numerical simulation

The Abaqus model consisted of a three-dimensional geometry of the CSB, using SHELL-type elements that represent the mid-surface of the plates, whose thickness is a property of the element. Web stiffeners were included at the supports and at the midspan to represent concentrated loads.

The numerical model simulates simply supported beams with two types of bracing: discrete and continuous. The discrete bracings developed are fork-type restraints at the supports and at midspan. To simulate the restraint, lateral displacements were restricted on the top and bottom flanges of the cross sections at the supports and midspan, vertical displacement was restricted at a point at the mid-height of each support's cross section, and longitudinal displacement was restricted at a point at the mid-height of one of the supports' cross section. The continuous bracing aims to prevent LTB (Lateral-Torsional Buckling), a common failure mode in larger beams, thereby promoting the manifestation of other mechanisms in numerical results.

The load was applied as a concentrated force on the top flange at midspan, using the modified Riks algorithm in Abaqus, which performs variable load increments controlled by numerical convergence criteria.The steel was modeled with a perfectly bilinear elastoplastic behavior, adopting a modulus of elasticity of 200 GPa and a Poisson's ratio of 0.3, according to ABNT NBR 8800:2024 [11]. In the plastic phase, stress remains constant, equal to the yield strength of 345 MPa (ASTM A572 Grade 50 steel). S4R and S3 element types were used, with free meshing. For short beams, fine meshes were adopted for better accuracy; for long beams, coarser meshes were used to reduce computational time and cost, as shown in Table 1.

The nonlinear numerical analysis is initiated with the deformation obtained from a prior buckling analysis, selecting the eigenvector with the lowest strain energy and its corresponding positive eigenvalue; this deformation is assigned an initial imperfection with a maximum amplitude equal to $d_g/100$. Residual stresses were considered using the distribution proposed by Vieira et al. [12].

Table 1. Mesh element size as a function of the span.

| Ratio $L_v/d_g$ | Element size (mm²) |
|---|---|
| $L_v/d_g \leq 3$ | 5 × 5 |
| $3 \leq L_v/d_g \leq 6$ | 10 × 10 |
| $6 \leq L_v/d_g \leq 20$ | 15 × 15 |
| $L_v/d_g \geq 20$ | 20 × 20 |

A parametric study was carried out to obtain results on load-carrying capacity and failure modes in CSB with the Litzka pattern, including 228 analyses of 12 different cross-sections and 12 different length-to-depth ratios, as shown in Board 1. For beams with $L_v/d_g \leq 6$, analyses were conducted using lateral bracing at midspan and at the supports. For beams with $L_v/d_g \geq 8$, analyses were performed with continuous bracing and also with bracing only at midspan and supports.

Board 1. Parameter variation (profile and span-to-depth ratio)

| **Profiles used** | | | | **Span-to-depth ratio** | | | |
|---|---|---|---|---|---|---|---|
| W250×17.9 | W310×21 | W360×32.9 | W460×52 | 2.5 | 5.0 | 10 | 20 |
| W250×25.3 | W310×28.3 | W360×51 | W460×82 | 3.0 | 6.0 | 12 | 25 |
| W250×44.8 | W310×52 | W360×79 | W460×97 | 4.0 | 8.0 | 15 | 30 |

# 3 Structural Reliability

The safety or failure of a structure has traditionally been quantified through its probability of failure Pf, that is, the probability that the effects of loads S exceed the structural resistance R. The reliability of a structure is defined as the complement of the probability of failure Pf, that is, C = 1 - Pf, and can be expressed in terms of a reliability index β. The target reliability index is the minimum established value for the reliability index, associated with a maximum failure probability that expresses the acceptable level of failure for the structure. The main criteria for defining the appropriate target reliability index are the consequences of failure and the costs of increasing reliability.

The mathematical relationships between β and Pf are defined by eq. (10).

$$\beta = -\Phi^{-1}(P_f). \tag{10}$$

Where $\Phi^{-1}$ is the inverse of the standard normal cumulative distribution function Φ.

One way to determine the probability of failure is through random sampling of the limit state function variables and calculating the probability using direct Monte Carlo simulation techniques. However, this method may require many simulations. For this reason, over the past decades, analytical methodologies such as the First Order Reliability Method (FORM) have been developed.

The main idea of FORM is that reliability can be easily obtained through a linear failure function by considering the space of statistically independent standardized variables, and by evaluating the shortest distance from the failure function to the origin (Hasofer and Lind [13]; Rackwitz and Fiessler [14]).

The failure function G(.) can be rewritten in terms of the nominal resistance ($R_n$), nominal values of dead load ($D_n$) and live load ($L_n$), as well as the normalized dimensionless random variables $\mathbf{R} = R/R_n$, $\mathbf{D} = D/D_n$ e $\mathbf{L} = L/L_n$. To avoid compromising the accuracy of the results when using a single variable R na análise de confiabilidade adota-s in the reliability analysis, $\mathbf{R} = \mathbf{MFP}$ is adopted. For convenience, normalized random variables are presented in bold. In eq. (11), the variable R depends on uncertainties related to material properties, cross-sectional geometry, and model error, represented by the normalized dimensionless variables **M** (material factor), **F** (fabrication factor) e **P** (professional factor), respectively.

$$G(.) = R_n\boldsymbol{MFP} - (D_n\boldsymbol{D} + L_n\boldsymbol{L}). \tag{11}$$

The design code criteria based on the limit state method can be expressed by eq. (12), when the structural component is subjected to a combination of gravitational loads (D + L).

$$\phi R_n \geq \gamma_D D_n + \gamma_L L_n. \tag{12}$$

Where $\phi$ is the resistance partial safety factor; γD is the dead load partial safety factor; and γL is the live load

partial safety factor.

The definition of the failure function G(.) for a component with known nominal resistance (Rn) applying ϕ, γD and γL transforms the design limit state equation into equality. $D_n$ e $L_n$ are obtained from eq. (13) and the definition of the load ratio (ρ = Ln/Dn).

$$D_n = \frac{\phi R_n}{\gamma_D + \rho\gamma_L}. \tag{13}$$

It is emphasized that in the Brazilian standard format and the Eurocode, the resistance partial safety factor $\phi$ is replaced by a factor γ greater than unity. Table 2 presents the resistance partial safety factors in terms of $\phi$ and γ, the partial safety factors for the design actions, and the load ratio between the usual loads in reliability studies of rolled profile beams.

Table 2. Partial safety factors of the code

| Code | $\phi$ or γ | γD | γL |
|---|---|---|---|
| AISC (LRFD) | 0.90 | 1.20 | 1.60 |
| Eurocode | 1.00 | 1.35 | 1.50 |
| NBR 8800 | 1.10 | 1.35 | 1.50 |

The original studies that determined the statistical properties (mean values and coefficients of variation) of the basic variables used to develop the provisions of the LRFD are presented in a series of papers in the September 1978 issue of the Journal of the Structural Division (ASCE, Vol. 104, ST9), one of which is by Ravindra and Galambos [15]. The corresponding statistics are provided in Galambos et al. [16]. Based on these statistics, the inherent β values in the Specification for the Design, Fabrication, and Erection of Structural Steel for Buildings (AISC [17]) were evaluated under different load combinations. As expected, there was considerable variation in the range of β values. For example, compact rolled beams (in bending) and tension members (in yielding) showed β values decreasing from approximately 3.1 at ρ = 0.50 to 2.4 at ρ = 5.

The Committee on Specifications defines a calibration ratio of ρ = 3.0 for the LRFD method, applied to compact beams in bending and tension members in yielding. The resistance factor ϕ for these ultimate strength limits is 0.90, and the corresponding β value is approximately 2.6 (AISC [18]).

### 3.1 Random Variables

The professional factor, **P**, is a random variable, whose analysis includes the uncertainties inherent in the model. It is the ratio between results obtained experimentally and theoretical results. The **P** factor provides information about the real performance of the model studied, revealing how conservative or insecure it is.

The statistical parameters of the variables **M**, **F**, **D** and **L** are shown in (Tab. 3) and were obtained from (Ellingwood et al. [19]). In reliability studies, it is usual to use the coefficient of variation, a measure of the dispersion of the variable in relation to the average value, in the analyses performed.

Table 3. Statistical data of the normalized random variables.

| Standardized Random Variable | Mean | Coefficient of Variation | Probability Distribuition Function |
|---|---|---|---|
| **M** | 1.10 | 0.10 | Lognormal |
| **F** | 1.00 | 0.05 | Lognormal |
| **D** | 1.05 | 0.10 | Normal |
| **L** | 1.00 | 0.25 | Gumbel |

# 4 Results

## 4.1 Professional Factor for WPB

Out of the 228 analyses performed, WPB occurred in 20 cases.

The professional factor **P**, also referred to as model error, was evaluated for this dataset using the Anderson-Darling statistical test, available in the MINITAB 19® software (MINITAB LLC [20]). It was found that the lognormal probability distribution function (PDF) provided a good fit to the datasets obtained from the ratio between the experimental result of each sample and its respective theoretical resistance. Table 4 presents the statistical data of the variable **P**, organized into two groups: $\gamma o = 1.25$ and $\gamma o$ from eq. (2).

Table 4. Statistical Analysis of the Professional Factor (Model Error)

| γo | Number of samples | Mean | Coefficient of variation | PDF |
|---|---|---|---|---|
| **1.25** | 20 | 1.157 | 0.054 | Lognormal |
| **Equation (2)** | 20 | 1.069 | 0.043 | Lognormal |

## 4.2 Realiability analysis for WPB

The structural reliability analysis conducted in this study allowed for the assessment of the safety of Litzka-type castellated beams, considering the effects of uncertainties in geometric parameters, material strength, loads, and calculation models. Resistance equations proposed in the literature were compared with results obtained from nonlinear numerical simulations using the finite element method. Figure 4 presents the results of the variation of the reliability index β as a function of the ratio ρ, considering both $\gamma o = 1.25$ and $\gamma o$ from eq. (2).

The curves show an average decrease in reliability of approximately 80% between $\rho = 0.5$ and $\rho = 5.0$. When $\rho = 3.0$, β is close to 2.6 [17] or higher. The Eurocode establishes a target reliability index of 3.8, but there is no clarity regarding the relationship of ρ in the calibration of this standard. This value is not reached within the ρ range of this study. It is observed that the introduction of the modified $\gamma_0$ reduces the conservatism of the design criterion for Litzka-type castellated beams.

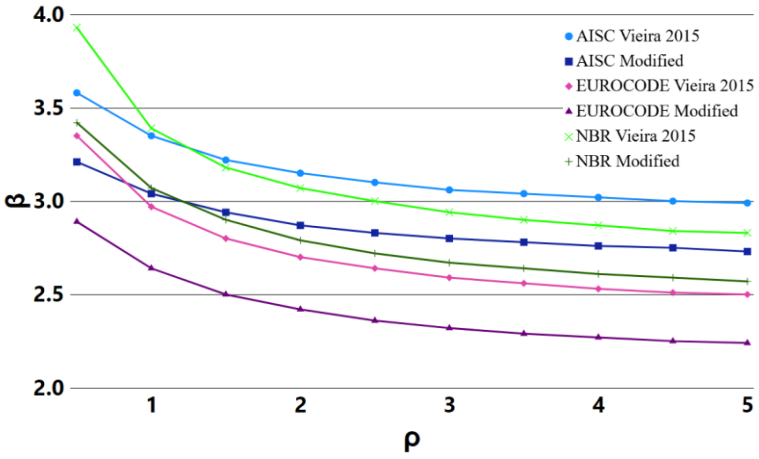



Figure 4. Reliability indices as a function of the load ratio.

# 5 Conclusions

The evaluation of the professional factor (model error) indicated that the modified $\gamma_0$ equation presents lower statistical dispersion and, therefore, greater representativeness of the results when compared to the equation with $\gamma_0 = 1.25$.

The reliability indices calculated using the FORM method, for different ρ ratios, demonstrated that the modified models (modified $\gamma_0$) exhibit a lower safety level compared to the models evaluated with $\gamma_0 = 1.25$, reducing the conservatism of the expressions.

Despite this, the reliability indices obtained for the modified models remain within acceptable ranges for commonly used structures (except for the Eurocode), according to reliability criteria established by international standards. It is worth emphasizing that the absence of a specific Brazilian standard for castellated beams reinforces the importance of studies like this, which contribute to the understanding of collapse mechanisms and the development of safer and more consistent design criteria aligned with the actual behavior of these structures.

It is recommended that future work explore the influence of other variables, such as different cellular patterns, aiming to broaden the scope of application of the proposed equations.

**Acknowledgements.** The authors are grateful to the Federal University of Itajuba (UNIFEI) and the National Council for Scientific and Technological Development (CNPq) for the support provided.

**Authorship statement.** The authors hereby confirm that they are the sole liable people responsible for the authorship of this work, and that all material that has been herein included as part of the present paper is either the property (and authorship) of the authors or has the permission of the owners to be included here.

## References

[1] Grünbauer, J. Accessed on 07/07/2025. Website: http://www.grunbauer.nl.
[2] Vieira, W. B. Estudo numérico-experimental da flambagem do montante de alma em vigas casteladas de aço. 2015. 105 f. Tese de Doutorado), Viçosa: UFV, 2015.
[3] Veríssimo, G. S.; Vieira, W. B.; Silveira, E. G.; Ribeiro, J. C. L; Paes, J. L. R.; Bezerra, E. M.; Silva, A. L. R. C.; Fakury, R. H.; Dimensionamento de vigas alveolares de aço. *Construmetal*. São Paulo, 2012.
[4] Oliveira, L. B.; Veríssimo, G. S.; Vieira, W. B.; Carvalho, J. M. F.; Paes, J. L. R. Procedimentos para definição das características geométricas de vigas alveolares de aço para sistemas de piso e de cobertura. *Construmetal*. São Paulo, 2012.
[5] Vieira, W. B. Simulação numérica do comportamento estrutural de vigas casteladas de aço com ênfase na flambagem do montante de alma. Dissertação de Mestrado, Viçosa: UFV, 2011.
[6] Gonçalves, A. B.; Ferrari, G. A.; Vieira, W. B; Paes, J. L. R.; Veríssimo, G. S.; Ribeiro, J. C. L.; Modelo numérico para avaliação do comportamento de vigas alveolares mistas de aço e concreto. *Construmetal*. São Paulo, 2014.
[7] Veríssimo, G. S.; Paes, J. L. R.; Fakury, R. H.; Rodrigues, F. C. Estudo de vigas de aço alveolares fabricadas a partir de perfis laminados brasileiros. Relatório de Pesquisa. Viçosa, UFV: 2010.
[8] Oliveira, L. B. Procedimentos para definição das características geométricas de vigas alveolares de aço para sistemas de piso e de cobertura. Dissertação de Mestrado, Viçosa: UFV, 2012.
[9] Pereira, B. G. F. H.; Rodrigues, M. A. R.; Vieira, W. B.; Brandão, A. L. R.; Veríssimo, G. S. Análise comparativa de custo de produção de vigas alveolares de aço em diferentes padrões. *Construmetal*. São Paulo, 2016.
[10] Kerdal, D.; Nethercot D. A. Failure modes for castellated beams. J. Constr. Steel Res. 295-315, 1984.
[11] Associação Brasileira de Normas Técnicas. NBR 8800. Projeto de Estruturas de Aço e de Estruturas Mistas de Aço e Concreto de Edifícios. Rio de Janeiro, 2024.
[12] Vieira, W. B; Veríssimo, G. S.; Ribeiro, J. C. L.; Paes, J. L. R. Simulação numérica do comportamento estrutural de vigas casteladas de aço com ênfase na flambagem do montante de alma. Ciência e Engenharia. Vol. 24: 105-113, 2015.
[13] Hasofer, A.M., Lind, N.C. Exact and invariant second-moment code format. Journal of the Engineering Mechanics division, 100(1), 111–121, 1974.
[14] Rackwitz, R. and Fiessler, B. Structural reliability under combined random load sequences, Computers and Structures, vol. 9, no. 5, pp. 489–494, 1978
[15] Ravindra, M.K., Galambos, T.V. Load and resistance factor design for steel. Journal of the Structural Division, ASCE, EUA, v. 104, n. ST9, 1978.
[16] Galambos, T.V.; Ellingwood, B.; Macgregor, J.G.; Cornell, C.A. Probability-based load criteria: assessment of current design practice. Journal of the Structural Division, Vol. 108, ST5, 959-977, 1982.
[17] AISC (1978), Specification for the Design, Fabrication, and Erection of Structural Steel for Buildings, American Institute of Steel Construction, Inc., Chicago, IL, 1978.
[18] AISC (2010). American National Standard. Specification for Structural Steel Building. AISC, Chicago, Illnois, Estados Unidos da América, 2010.
[19] Ellingwood, B.; Macgregor, J. G.; Galambos, T. V.; Cornell, C. A. Development of a Probability-Based Load Criterion for American National Standard A58. NBS Special Publication 577, National Bureau of Standards, United States Department of Commerce, Washington, D.C., Estados Unidos da América, 1980.
[20] Minitab, LLC. (2019). Minitab 19 Statistical Software (Version 19). Minitab, LLC.